Governance and COVID-19 Cases/Deaths in 180 Different Countries: Spin-Glass-Chaos Complexity Classification and Clustering

Izzet S. Darendeli,[1] Alpar Türkoğlu,[2,3] Ibrahim Keçoğlu,[3,4] E. Can Artun,[5,6] and A. Nihat Berker[6,5,7]

[1] *Department of Management, California State University, East Bay, California 94607, USA*
[2] *Department of Electrical and Electronics Engineering, Boğaziçi University, Bebek, Istanbul 34342, Turkey*
[3] *Department of Physics, Boğaziçi University, Bebek, Istanbul 34342, Turkey*
[4] *Department of Mathematics, Boğaziçi University, Bebek, Istanbul 34342, Turkey*
[5] *TÜBITAK Research Institute for Fundamental Sciences, Gebze, Kocaeli 41470, Turkey*
[6] *Faculty of Engineering and Natural Sciences, Kadir Has University, Cibali, Istanbul 34083, Turkey*
[7] *Department of Physics, Massachusetts Institute of Technology, Cambridge, Massachusetts 02139, USA*

A complexity classification scheme, recently developed from the fractal spectra of adjustable spin-glass chaos, is applied to COVID19-Governance correlations of 180 nations. Corruption, political stability, absence of violence/terrorism, voice and accountability, government response, and government-response time, as governance indicators, are correlated and clustered with COVID-19 cases and deaths between 1 January 2020 and 27 February 2022 in 180 countries. Systematic patterns and tell-tale clusterings are found to emerge.

I. INTRODUCTION: SPIN-GLASS CHAOS AS A COVID19-GOVERNANCE COMPLEXITY CLASSIFICATION SCHEME

The COVID-19 pandemic has inarguably been the most planet-shaking occurrence of modern memory. Furthermore, by imbibing to the differing social mores and differing governances of different countries, the pandemic has proceeded quite differently. This variegation has provided a distribution of archetypical complexity that requires communally vital understanding and analysis, which need be quantitative to be widely and quickly useful.

Such a flexible and widely applicable method has recently been developed from statistical physics.[1] Spin-glasses, which are magnetic systems with competing local interactions, typically enter a phase that shows temperature chaos [2, 3] under successive scale changes. The fractal spectrum is a readily obtained quantitative signature of this complex behavior. Furthermore, spin-glasses on hierarchical lattices [4–6] are exactly solved and the family of hierarchical lattices provides a continuum of complexity types that match and categorize actual systems, thus revealing clustering and systematics. This scheme has been quantitatively demonstrated [1] with multicultural multigeographic music and with brain signals [7–11].

Similarly, in the current work, important information is obtained on governance through the (unfortunate) litmus paper of the COVID-19 pandemic.

II. COVID-19 AND GOVERNANCE DATA IN 180 COUNTRIES

Data for our multifractal spin-glass-chaos projection method was acquired from the Oxford COVID-19 Government Response Tracker (OxCGRT)[12]. The data set consists of confirmed daily incidences and deaths due to COVID-19. Daily confirmed incidences and deaths due to COVID-19 cases constitute sets of time series which are complex and show fractal behavior. This very nature of the data makes it suitable to be analyzed via our method.

To correlate with COVID-19, we obtained governance indicators and GNI per capita for each country from the World Bank open database [13]. These data differentiate the countries in terms of governance and income. The governance indicators are control of corruption, political stability, absence of violence/terrorism, voice and accountability, government response, and government-response time. The countries were separated into four levels of income: low, lower-middle, upper-middle, and high income. All of our data were accessed as of February 27, 2022. There are 186 countries with daily COVID-19 data which OxCGRT provides. In the OxCGRT database there is also government response data. One of the countries lacked this data; therefore, we discarded it. On the other hand, the World Bank provides governance indicators for 214 countries, ten of which lack data for some indicators. Therefore we have discarded these ten countries and took the intersection of the remaining set and the set of countries in the COVID-19 data. Thus 180 countries were left, after the intersection, for our analysis.

III. A WIDELY APPLICABLE AND FLEXIBLE CLUSTERING OF COMPLEXITY FROM SPIN-GLASS CHAOS

The classification method that we use [1] fits the data to a chaotic spin glass in terms of multifractality and finally represents it as a single point in the multiparameter space of the hierarchical lattices on which the Ising spin glasses are lodged. Each data series hence can be seen as a single point in the model parameter space as in Figs.

1 and 2. Classification is achieved by labeling the data series according to the governance categories and observing the possible patterns and relations within and across the categories that the points reflect in the scatter plots. We took each data series of confirmed daily incidences and deaths related to COVID-19 for each country as a time series and calculated the multifractal spectrum, also called singularity spectrum, of each time series by using the Chhabra-Jensen algorithm [14]. Then we searched for a specific spin-glass system such that the multifractal spectrum of its chaotic renormalization-group trajectory best fits the spectrum of the corresponding data series. The detailed calculations are presented in [1, 3]. To obtain the spin-glass chaos projection, we used Ising spin systems on frustrated hierarchical lattices [4–6] that are exactly solved. The analysis applied finds an analogical Ising system in terms of multifractal characteristics for the given data. Using this, we can scatter the given data onto the parameter space of the Ising model. Consequently, a classification can be made among the data of different categories.

IV. RESULTS

We present the spin-glass-chaos projection results for confirmed daily cases and deaths due to COVID-19 per country in Figs. 1 and 2, respectively. Every colored point in the figures corresponds to the spin-glass-chaos projection of the data of a country. Points may have different radii; this is only to avoid overlapping points to become invisible. Each panel in the two figures shows the projection results of the countries in relation to the corresponding governance indicator specified in the titles of the panels. Since there is no direct relation between spin-glass models and the data given, because the former solely underpins a classification method, a point in the scatter plots has no meaning by standing alone. On the other hand, the results manifest important meaning in relation to each other. The points, hence the countries, in the panels are colored with respect to the quartile they fall into.

Two main clusters can be identified as they are specified by the dashed boxes. The country names are added with colors reflecting their income levels. All country names are grouped in Figs. 3 and 4. Three types of observations lead to discussion and results: (i) the geometric positions and evident clustering of countries, (ii) the colors of the points in each panel, reflecting quartiles in five different governance characteristics, (iii) the colors of the country names, reflecting quartiles in income. Even though the locations of these points are the same throughout the panels (reflecting case or death statistics), they generally differ between Fig. 1 and 2.

The color of the points shows the quartile of the country for the governance indicator indicated at the top of the figure. The color of the country name shows the income quartile. For example, a lower left point in panels of Fig. 1 stands for Kuwait, the different colors in panels indicating that this country falls into different quartiles for the different governance indicators. The purple color of the Kuwait country name shows that Kuwait is a country with high-income level in terms of GNI per capita. Surprisingly in Fig. 2, Kuwait appears shifted to the lower middle, thus with a different position than in Fig. 1. This reflects the dissimilarity between regulations and fluctuations, or multifractality, in daily cases and deaths due to COVID-19 in Kuwait between 1 January 2020 and 27 February 2022. There are countries that show greater or smaller differences in daily cases and deaths of COVID-19, that is, the distances between the points of the countries in Figs. 1 and 2 are greater or smaller. Fig. 5 shows these distances of each country on a world map. There are also points, that is, countries, that have overlapping point locations in Figs.1 and/or 2. These "overlapping" countries are also shown on a world map in Figs. 6 and 7, respectively for Figs. 1 and 2, as separate groups for each overlap point.

It is thus seen that all of the governance indicators equally affect COVID-19 performance. There is a general pattern emerging from all ten spin-glass-chaos projection points: For both cases and deaths, for all five governance indicators, there is a cluster of purple-yellow (high-uppermiddle governance) points in the top regions of the panels which shows a diagonal line pattern, occurring in each panel. The purple color corresponds to the fourth quartile (Q4), which is the highest quartile of the corresponding indicator. Furthermore, orange and yellow points (lowermiddle-uppermiddle governance) dominate the horizontal clusters at the bottom of Figs. 1 and 2.

In Figs. 1, 2, and in Figs. 3, 4 for all 180 countries, the country names are colored according to their GNI per capita: blue for low, orange for lower-middle, yellow for higher-middle, and purple for high-income level. (Thus, point and country-name color coding respectively for both five governance indicators and income are the same.) The relation between governance and income level shows a complex pattern. There are countries, such as Saudi Arabia, Belarus, and Italy, that fall into different quartiles for different governance indicators, showing that there is no necessary deterministic relation among the governance indicators on a specific country basis. However, one may expect to see countries that fall into the same quartile to be represented by nearer points, that is, to see points with the same color near to each other. This is partially confirmed, that is, points with the same color are clustered not altogether in a whole panel, but showing a set of subclusters. In both Figs. 3 and 4, the results for the control of corruption, political stability and absence of violence/terrorism, and voice and accountability are more similar to each other but differ from the other two indicators: The highest income countries strongly dominate the highest quartile governance. Conversely, the results for government response and government response time resemble each other more than they do the others, as the highest income quantities do

not distinguish themselves in response governance indicators.

The other surprising result is that some of the points have the same coordinates in the parameter space, that is, COVID-19 performances of some countries resemble each other in terms of multifractality and show the exact same spin-glass-chaos projections. These overlapping points constitute 4 groups of parameter values. For confirmed daily incidences due to COVID-19, best fitting parameters are $m_1 = 36.2, p_b = 73.8$ for Group 1, $m_1 = 11.1, p_b = 157.4$ for Group 2, $m_1 = 11.6, p_b = 174.9$ for Group 3, $m_1 = 15.1, p_b = 189.3$ for Group 4. For daily deaths due to COVID-19, best fitting parameters are $m_1 = 9.5, p_b = 195.7$ for Group 1, $m_1 = 15.1, p_b = 189.3$ for Group 2, $m_1 = 13.9, p_b = 196.2$ for Group 3, $m_1 = 14.0, p_b = 197.3$ for Group 4. Figs. 6 and 7 show some of many countries that have these same projections in Figs. 1 and 2, respectively. There seem to be neither geographical nor cultural correlation between countries that fall into the same groups in Fig. 6, which shows the overlapping results for the confirmed daily incidences due to COVID-19. In Fig. 7, on the other hand, there seems to be groupings of south and middle, with countries which are geographically and culturally similar to each other falling into the same group. But, for instance, countries in Group 3 are very different from each other in many aspects including income level and governance.

A comparison between the projection results of confirmed incidences and deaths due to COVID-19 for each country is shown in Fig. 5. Normalized Euclidean distances in the range [0,1] between points of Figs. 1 and 2 for each country are calculated and presented on the world map. Countries colored with lighter blue are those which showed similar fluctuation patterns and fractal spectrum in the course of daily confirmed incidences and deaths due to COVID-19. Countries with darker blue tones are those which have projection results for the courses of daily cases and deaths more distant from each other.

Some of them are also highlighted with colors at the borders of the countries according to their income levels. For example, Indonesia and Guinée have similar distances between their projection results in their courses of daily cases and deaths, although the first is a lower-middle-income country and the latter is a low-income country. Another interesting comparison can be made between Russia and Turkey. There are aspects that differ from each other, such as size, population, and military power. On the other hand, there are aspects that resemble each other, such as governance and income level. They have similar projection results for the distances of daily cases and deaths.

V. CONCLUSION

ACKNOWLEDGMENTS

Support by the Academy of Sciences of Turkey (TÜBA) is gratefully acknowledged.

[1] E. C. Artun, I. Keçoğlu, A. Türkoğlu, and A. N. Berker, Multifractal Spin-Glass Chaos Projection and Interrelation of Multicultural Music and Brain Signals, arXiv:2201.10261 [cond-mat.dis-nn] (2022).

[2] S. R. McKay, A. N. Berker, and S. Kirkpatrick, Spin-Glass Behavior in Frustrated Ising Models with Chaotic Renormalization-Group Trajectories, Phys. Rev. Lett. **48**, 767 (1982).

[3] A. Türkoğlu and A. N. Berker, Frustrated Potts: Multiplicity Eliminates Chaos via Reentrance, Phys. Rev. E **102**, 022122 (2020).

[4] A. N. Berker and S. Ostlund, Renormalisation-Group Calculations of Finite Systems: Order Parameter and Specific Heat for Epitaxial Ordering, J. Phys. C **12**, 4961 (1979).

[5] R. B. Griffiths and M. Kaufman, Spin Systems on Hierarchical Lattices: Introduction and Thermodynamic Limit, Phys. Rev. B **26**, 5022R (1982).

[6] M. Kaufman and R. B. Griffiths, Spin Systems on Hierarchical Lattices: 2. Some Examples of Soluble Models, Phys. Rev. B **30**, 244 (1984).

[7] M. Torkamani-Azar, S. D. Kanik, S. Aydın and M. Çetin, Prediction of Reaction Time and Vigilance Variability from Spatio-Spectral Features of Resting-State EEG in a Long Sustained Attention Task, IEEE J. Biomedical and Health Informatics, **24** 2550, (2020).

[8] I. Daly, N. Nicolaou, D. Williams, F. Hwang, A. Kirke, E. Miranda, and S. J. Nasuto (2021), An EEG Dataset Recorded during Affective Music Listening, OpenNeuro, [Dataset] doi: 10.18112/openneuro.ds002721.v1.0.2 (2021).

[9] P. Kraemer, EEG **10**, 20. Zenodo. https://doi.org/10.5281/zenodo.3926093 (2020).

[10] R. Oostenveld, P. Fries, E. Maris, and J.-M. Schoffelen, FieldTrip: Open Source Software for Advanced Analysis of MEG, EEG, and Invasive Electrophysiological Data, Computational Intelligence Neuroscience **2011**, e156869 (2010).

[11] L. G. S. França, J. G. V. Miranda, M. Leite, N. K. Sharma, M. C. Walker, L. Lemieux, and Y. Wang, Fractal and Multifractal Properties of Electrographic Recordings of Human Brain Activity: Toward Its Use as a Signal Feature for Machine Learning in Clinical Applications, Frontiers in Physiology **9**, 01767 (2018).

[12] T. Hale, N. Angrist, R. Goldszmidt, B. Kira, A. Petherick, T. Phillips, S.Webster, E. Cameron-Blake, L. Hallas, S. Majumdar, and H. Tatlow, A Global Panel Database of Pandemic Policies, Oxford Covid-19 Government Response Tracker (2021).

[13] World Bank Databank, Control of Corruption: Percentile Rank Political Stability and Absence of Violence/Terrorism, Voice and Accountability, Governance Indicators (2022).

[14] A. Chhabra and R. V. Jensen, Direct Determination of

the f(α) Singularity Spectrum, Phys. Rev. Lett. **62**, 1327 (1989).

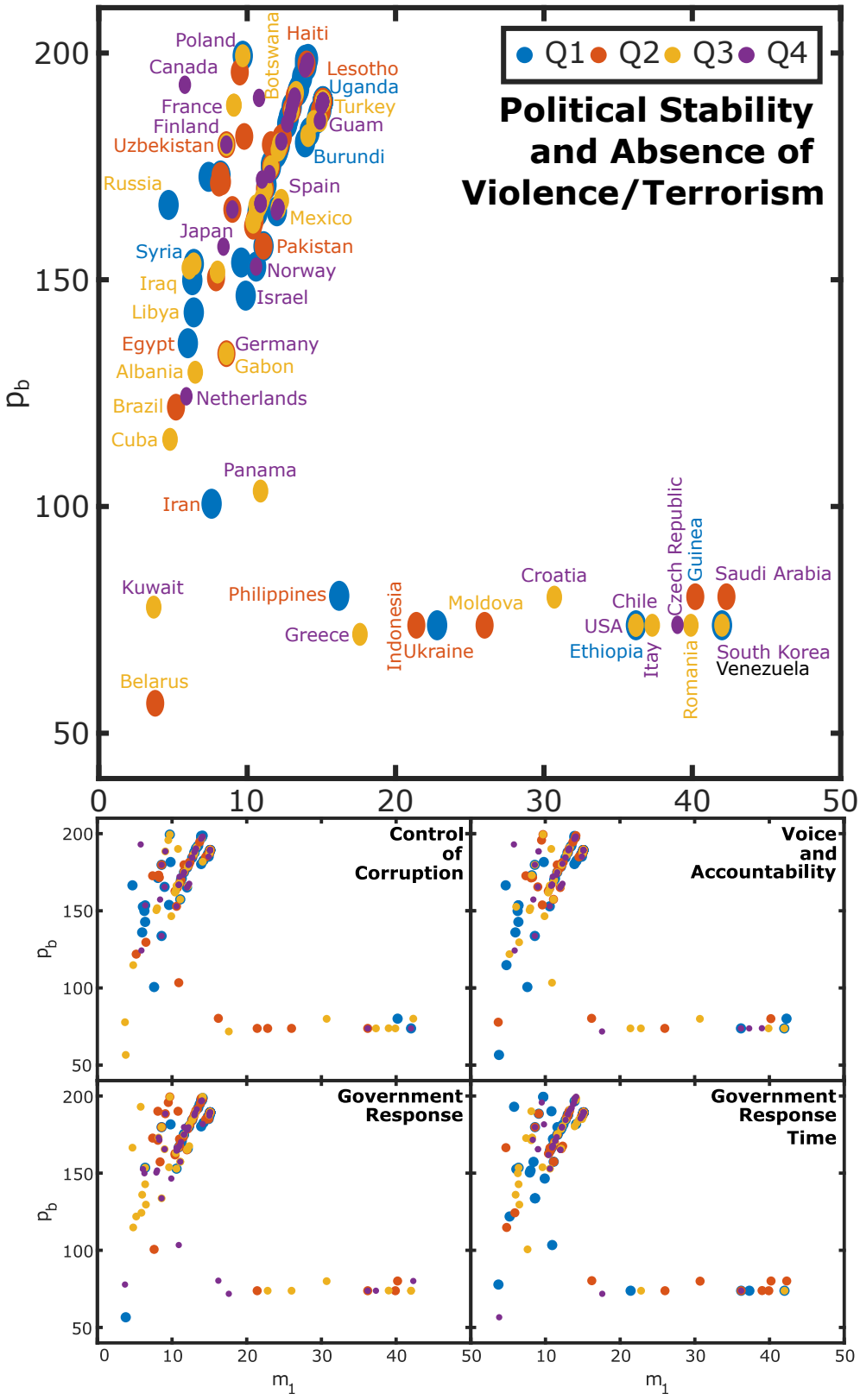

FIG. 1. Scatter plots of the best fitting spin-glass chaos parameters for daily COVID-19 cases per country. The location of each country is the same in all five panels in this figure. For each country, the point is colored according to the quartile of the governance characteristic specified in the panel. The country names are colored according to the GNI per capita categories. For both point-coloring and name-coloring, the quartiles are colored blue, orange, yellow, and purple, for low, lower-middle, upper-middle, and high quartiles/categories, respectively.

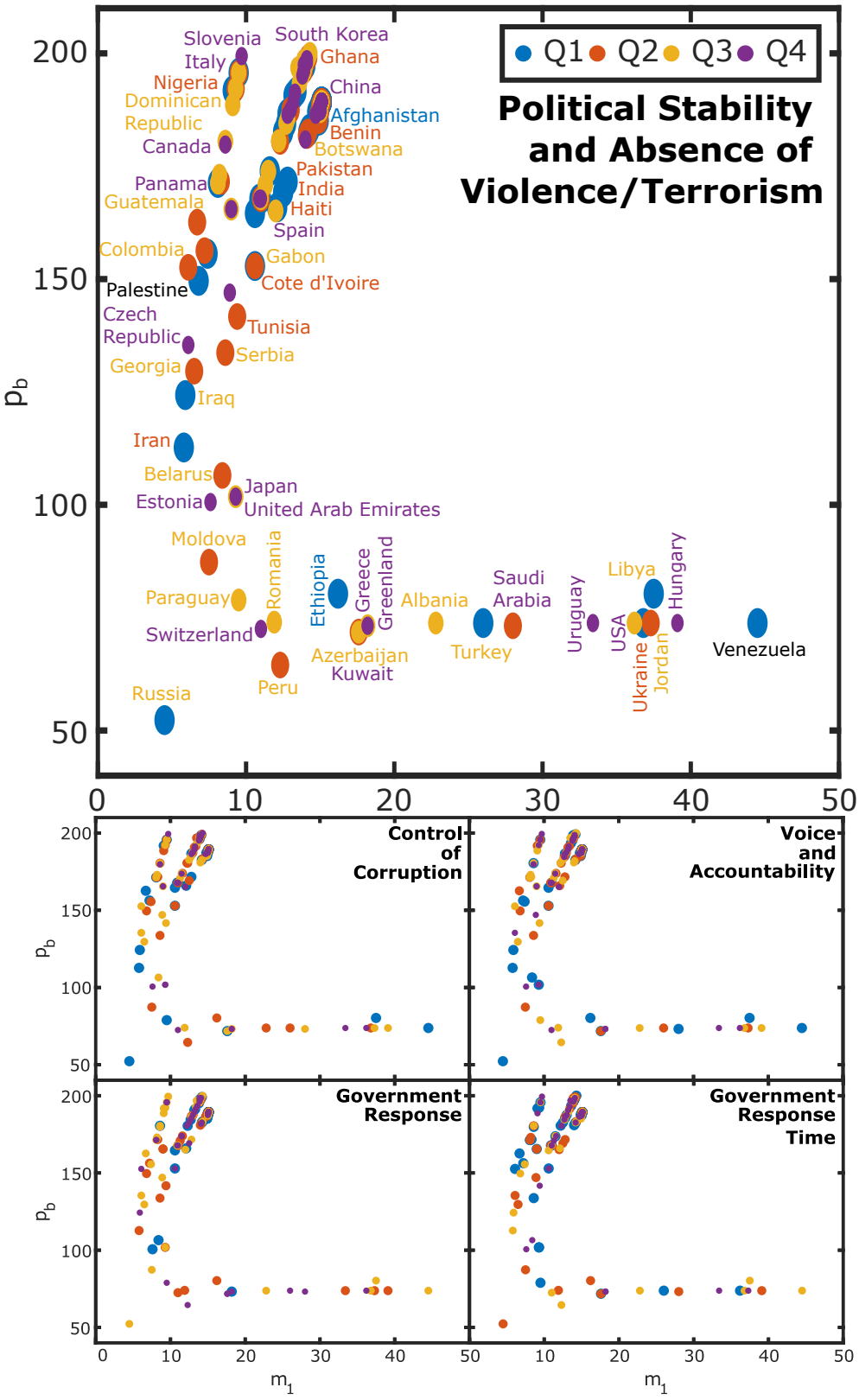

FIG. 2. Scatter plots of the best fitting spin-glass chaos parameters for daily COVID-19 deaths per country. The location of each country is the same in all five panels in this figure (but in general different than in Fig. 2). For each country, the point is colored according to the quartile of the governance characteristic specified in the panel. The country names are colored according to the GNI per capita categories. For both point-coloring and name-coloring, the quartiles are colored blue, orange, yellow, and purple, for low, lower-middle, upper-middle, and high quartiles/categories, respectively.

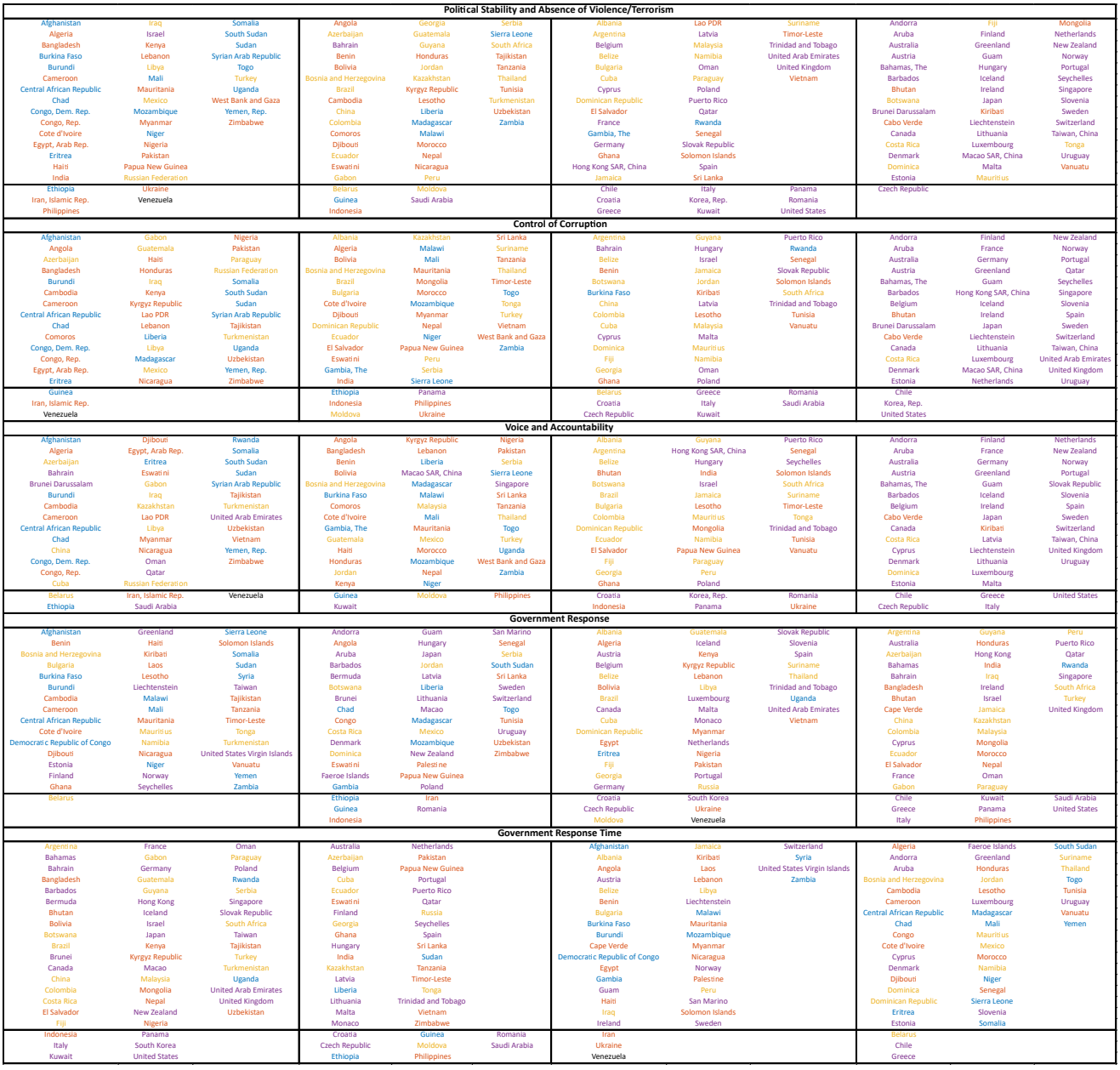

FIG. 3. Country lists for daily COVID-19 cases, separated into the two clusters (Fig. 1) of each governance indicator. The upper and lower clusters of Fig. 1 are given as upper and lower rows under each governance indicator. The country name-coloring, by income, is blue, orange, yellow, and purple, for low, lower-middle, upper-middle, and high categories, respectively.

Political Stability and Absence of Violence/Terrorism											
Afghanistan	Haiti	Nigeria	Angola	Gabon	Morocco	Argentina	Ghana	Qatar	Andorra	Denmark	Mauritius
Algeria	India	Pakistan	Bahrain	Georgia	Nepal	Belgium	Hong Kong SAR, China	Rwanda	Aruba	Dominica	Mongolia
Bangladesh	Iran, Islamic Rep.	Papua New Guinea	Benin	Guatemala	Nicaragua	Belize	Italy	Senegal	Australia	Fiji	Netherlands
Burkina Faso	Iraq	Philippines	Bolivia	Guinea	Serbia	Bulgaria	Jamaica	Slovak Republic	Austria	Finland	New Zealand
Burundi	Israel	Somalia	Bosnia and Herzegovina	Guyana	Sierra Leone	Chile	Korea, Rep.	Solomon Islands	Bahamas, The	Guam	Norway
Cameroon	Kenya	South Sudan	Brazil	Honduras	South Africa	Croatia	Lao PDR	Spain	Barbados	Iceland	Portugal
Central African Republic	Lebanon	Sudan	Cambodia	Indonesia	Tajikistan	Cuba	Latvia	Sri Lanka	Bhutan	Ireland	Seychelles
Chad	Mali	Syrian Arab Republic	China	Kazakhstan	Tanzania	Cyprus	Malaysia	Suriname	Botswana	Kiribati	Singapore
Congo, Dem. Rep.	Mauritania	Togo	Colombia	Kyrgyz Republic	Thailand	Dominican Republic	Namibia	Timor-Leste	Brunei Darussalam	Liechtenstein	Slovenia
Congo, Rep.	Mexico	Uganda	Comoros	Lesotho	Tunisia	El Salvador	Oman	Trinidad and Tobago	Cabo Verde	Lithuania	Sweden
Cote d'Ivoire	Mozambique	West Bank and Gaza	Djibouti	Liberia	Turkmenistan	France	Panama	United Kingdom	Canada	Luxembourg	Taiwan, China
Egypt, Arab Rep.	Myanmar	Yemen, Rep.	Ecuador	Madagascar	Uzbekistan	Gambia, The	Poland	Vietnam	Costa Rica	Macao SAR, China	Tonga
Eritrea	Niger	Zimbabwe	Eswatini	Malawi	Zambia	Germany	Puerto Rico		Czech Republic	Malta	Vanuatu
Ethiopia	Turkey		Azerbaijan	Moldova		Albania	Paraguay	United States	Estonia	Japan	
Libya	Ukraine		Belarus	Peru		Greece	Romania		Greenland	Switzerland	
Russian Federation	Venezuela		Jordan	Saudi Arabia		Kuwait	United Arab Emirates		Hungary	Uruguay	
Control of Corruption											
Afghanistan	Guatemala	Nigeria	Algeria	Kazakhstan	Sierra Leone	Argentina	Georgia	Poland	Andorra	Finland	Norway
Angola	Guinea	Pakistan	Bolivia	Malawi	Sri Lanka	Bahrain	Ghana	Puerto Rico	Aruba	France	Portugal
Bangladesh	Haiti	Somalia	Bosnia and Herzegovina	Mali	Suriname	Belize	Guyana	Rwanda	Australia	Germany	Qatar
Burundi	Honduras	South Sudan	Brazil	Mauritania	Tanzania	Benin	Israel	Senegal	Austria	Guam	Seychelles
Cambodia	Iran, Islamic Rep.	Sudan	Bulgaria	Mongolia	Thailand	Botswana	Italy	Slovak Republic	Bahamas, The	Hong Kong SAR, China	Singapore
Cameroon	Iraq	Syrian Arab Republic	Cote d'Ivoire	Morocco	Timor-Leste	Burkina Faso	Jamaica	Solomon Islands	Barbados	Iceland	Slovenia
Central African Republic	Kenya	Tajikistan	Djibouti	Mozambique	Togo	China	Kiribati	South Africa	Belgium	Ireland	Spain
Chad	Kyrgyz Republic	Turkmenistan	Dominican Republic	Myanmar	Tonga	Colombia	Latvia	Trinidad and Tobago	Bhutan	Korea, Rep.	Sweden
Comoros	Lao PDR	Uganda	Ecuador	Nepal	Vietnam	Croatia	Lesotho	Tunisia	Brunei Darussalam	Liechtenstein	Taiwan, China
Congo, Dem. Rep.	Lebanon	Uzbekistan	El Salvador	Niger	West Bank and Gaza	Cuba	Malaysia	Vanuatu	Cabo Verde	Lithuania	United Kingdom
Congo, Rep.	Liberia	Yemen, Rep.	Eswatini	Panama	Zambia	Cyprus	Malta		Canada	Luxembourg	
Egypt, Arab Rep.	Madagascar	Zimbabwe	Gambia, The	Papua New Guinea		Czech Republic	Mauritius		Chile	Macao SAR, China	
Eritrea	Mexico		India	Philippines		Dominica	Namibia		Costa Rica	Netherlands	
Gabon	Nicaragua		Indonesia	Serbia		Fiji	Oman		Denmark	New Zealand	
Azerbaijan	Russian Federation		Albania	Peru		Belarus	Jordan	Saudi Arabia	Estonia	Switzerland	Uruguay
Libya	Venezuela		Ethiopia	Turkey		Greece	Kuwait		Greenland	United Arab Emirates	
Paraguay			Moldova	Ukraine		Hungary	Romania		Japan	United States	
Voice and Accountability											
Afghanistan	Egypt, Arab Rep.	South Sudan	Angola	Kyrgyz Republic	Nigeria	Argentina	Guyana	Puerto Rico	Andorra	Dominica	Netherlands
Algeria	Eritrea	Sudan	Bangladesh	Lebanon	Pakistan	Belize	Hong Kong SAR, China	Senegal	Aruba	Finland	New Zealand
Bahrain	Eswatini	Syrian Arab Republic	Benin	Liberia	Philippines	Bhutan	India	Seychelles	Australia	France	Norway
Brunei Darussalam	Gabon	Tajikistan	Bolivia	Macao SAR, China	Serbia	Botswana	Indonesia	Solomon Islands	Austria	Germany	Portugal
Burundi	Iran, Islamic Rep.	Turkmenistan	Bosnia and Herzegovina	Madagascar	Sierra Leone	Brazil	Israel	South Africa	Bahamas, The	Guam	Slovak Republic
Cambodia	Iraq	Uzbekistan	Burkina Faso	Malawi	Singapore	Bulgaria	Jamaica	Suriname	Barbados	Iceland	Slovenia
Cameroon	Kazakhstan	Vietnam	Comoros	Malaysia	Sri Lanka	Colombia	Korea, Rep.	Timor-Leste	Belgium	Ireland	Spain
Central African Republic	Lao PDR	Yemen, Rep.	Cote d'Ivoire	Mali	Tanzania	Croatia	Lesotho	Tonga	Cabo Verde	Italy	Sweden
Chad	Myanmar	Zimbabwe	Gambia, The	Mauritania	Thailand	Dominican Republic	Mauritius	Trinidad and Tobago	Canada	Kiribati	Taiwan, China
China	Nicaragua		Guatemala	Mexico	Togo	Ecuador	Mongolia	Tunisia	Chile	Latvia	United Kingdom
Congo, Dem. Rep.	Oman		Guinea	Morocco	Uganda	El Salvador	Namibia	Vanuatu	Costa Rica	Liechtenstein	
Congo, Rep.	Qatar		Haiti	Mozambique	West Bank and Gaza	Fiji	Panama		Cyprus	Lithuania	
Cuba	Rwanda		Honduras	Nepal	Zambia	Georgia	Papua New Guinea		Czech Republic	Luxembourg	
Djibouti	Somalia		Kenya	Niger		Ghana	Poland		Denmark	Malta	
Azerbaijan	Libya	United Arab Emirates	Jordan	Turkey		Albania	Peru		Estonia	Japan	Uruguay
Belarus	Russian Federation	Venezuela	Kuwait			Hungary	Romania		Greece	Switzerland	
Ethiopia	Saudi Arabia		Moldova			Paraguay	Ukraine		Greenland	United States	
Government Response											
Afghanistan	Kiribati	Somalia	Andorra	Guam	San Marino	Algeria	Germany	Slovenia	Argentina	Guyana	Panama
Benin	Laos	Sudan	Angola	Guinea	Senegal	Austria	Guatemala	South Korea	Australia	Honduras	Philippines
Bosnia and Herzegovina	Lesotho	Syria	Aruba	Indonesia	Serbia	Belgium	Iceland	Spain	Bahamas	Hong Kong	Puerto Rico
Bulgaria	Liechtenstein	Taiwan	Barbados	Iran	South Sudan	Belize	Kenya	Suriname	Bahrain	India	Qatar
Burkina Faso	Malawi	Tajikistan	Bermuda	Latvia	Sri Lanka	Bolivia	Kyrgyz Republic	Thailand	Bangladesh	Iraq	Rwanda
Burundi	Mali	Tanzania	Botswana	Liberia	Sweden	Brazil	Lebanon	Trinidad and Tobago	Bhutan	Ireland	Singapore
Cambodia	Mauritania	Timor-Leste	Brunei	Lithuania	Togo	Canada	Luxembourg	Uganda	Cape Verde	Israel	South Africa
Cameroon	Mauritius	Tonga	Chad	Macao	Tunisia	Croatia	Malta	Vietnam	Chile	Italy	United Kingdom
Central African Republic	Namibia	Turkmenistan	Congo	Madagascar	Uzbekistan	Cuba	Monaco		China	Jamaica	
Cote d'Ivoire	Nicaragua	United States Virgin Islands	Costa Rica	Mexico	Zimbabwe	Czech Republic	Myanmar		Colombia	Kazakhstan	
Democratic Republic of Congo	Niger	Vanuatu	Denmark	Mozambique		Dominican Republic	Netherlands		Cyprus	Malaysia	
Djibouti	Norway	Yemen	Dominica	New Zealand		Egypt	Nigeria		Ecuador	Mongolia	
Finland	Seychelles	Zambia	Eswatini	Palestine		Eritrea	Pakistan		El Salvador	Morocco	
Ghana	Sierra Leone		Faeroe Islands	Papua New Guinea		Fiji	Portugal		France	Nepal	
Haiti	Solomon Islands		Gambia	Poland		Georgia	Slovak Republic		Gabon	Oman	
Belarus			Ethiopia	Jordan	Uruguay	Albania	Russia	Venezuela	Azerbaijan	Paraguay	Turkey
Estonia			Hungary	Romania		Libya	Ukraine		Greece	Peru	United States
Greenland			Japan	Switzerland		Moldova	United Arab Emirates		Kuwait	Saudi Arabia	
Government Response Time											
Argentina	France	Nigeria	Australia	Monaco	Zimbabwe	Afghanistan	Jamaica	Zambia	Algeria	Faeroe Islands	Thailand
Bahamas	Gabon	Oman	Belgium	Netherlands		Angola	Kiribati		Andorra	Honduras	Togo
Bahrain	Germany	Panama	Croatia	Pakistan		Austria	Laos		Aruba	Lesotho	Tunisia
Bangladesh	Guatemala	Poland	Cuba	Papua New Guinea		Belize	Lebanon		Bosnia and Herzegovina	Luxembourg	Vanuatu
Barbados	Guyana	Rwanda	Czech Republic	Philippines		Benin	Liechtenstein		Cambodia	Madagascar	Yemen
Bermuda	Hong Kong	Serbia	Ecuador	Portugal		Bulgaria	Malawi		Cameroon	Mali	
Bhutan	Iceland	Singapore	Eswatini	Puerto Rico		Burkina Faso	Mauritania		Central African Republic	Mauritius	
Bolivia	Indonesia	Slovak Republic	Finland	Qatar		Burundi	Mozambique		Chad	Mexico	
Botswana	Israel	South Africa	Georgia	Seychelles		Cape Verde	Myanmar		Chile	Morocco	
Brazil	Italy	South Korea	Ghana	Spain		Democratic Republic of Congo	Nicaragua		Congo	Namibia	
Brunei	Kenya	Taiwan	Guinea	Sri Lanka		Egypt	Norway		Cote d'Ivoire	Niger	
Canada	Kyrgyz Republic	Tajikistan	India	Sudan		Gambia	Palestine		Cyprus	Senegal	
China	Macao	Turkmenistan	Kazakhstan	Tanzania		Guam	San Marino		Denmark	Sierra Leone	
Colombia	Malaysia	Uganda	Latvia	Timor-Leste		Haiti	Solomon Islands		Djibouti	Slovenia	
Costa Rica	Mongolia	United Kingdom	Liberia	Tonga		Iran	Sweden		Dominica	Somalia	
El Salvador	Nepal	Uzbekistan	Lithuania	Trinidad and Tobago		Iraq	Syria		Dominican Republic	South Sudan	
Fiji	New Zealand		Malta	Vietnam		Ireland	United States Virgin Islands		Eritrea	Suriname	
Japan	Turkey		Azerbaijan	Moldova	Saudi Arabia	Albania	Switzerland		Belarus	Greenland	
Kuwait	United Arab Emirates		Ethiopia	Romania		Libya	Ukraine		Estonia	Jordan	
Paraguay	United States		Hungary	Russia		Peru	Venezuela		Greece	Uruguay	

FIG. 4. Country lists for daily COVID-19 deaths, separated into the two clusters (Fig. 2) of each governance indicator. The upper and lower clusters of Fig. 2 are given as upper and lower rows under each governance indicator. The country name-coloring, by income, is blue, orange, yellow, and purple, for low, lower-middle, upper-middle, and high categories, respectively.

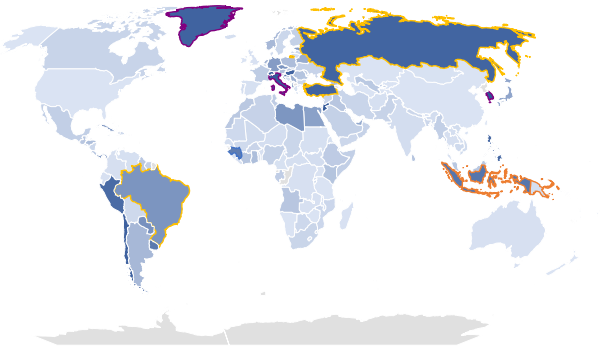

FIG. 5. Map of normalized Euclidean distances between points of Figs. 1 and 2 for each country. Countries that are discussed in the text are highlighted with colors according to GNI per capita, blue, orange, yellow, purple standing for low, lower-middle, upper-middle, and high income, respectively.

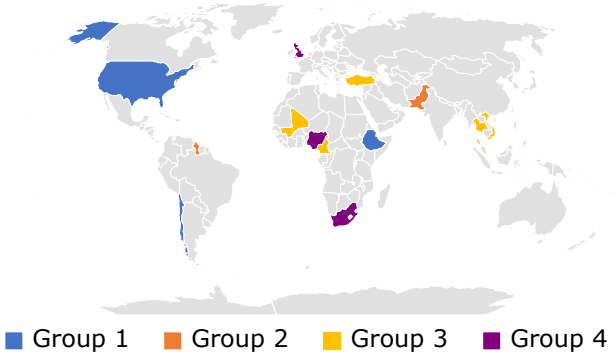

FIG. 6. Distribution of some of the countries that are overlapping in Fig. 1. Colors indicate different overlap points in the scatter plot: Group 1: $m_1 = 36.2, p_b = 73.8$; Group 2: $m_1 = 11.1, p_b = 157.4$; Group 3: $m_1 = 11.6, p_b = 174.9$; Group 4: $m_1 = 15.1, p_b = 189.3$.

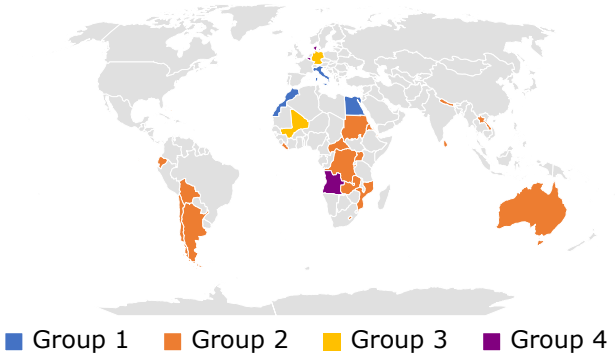

FIG. 7. Distribution of some of the countries that are overlapping in Fig. 2. Colors indicate different overlap points in the scatter plot: Group 1: $m_1 = 9.5, p_b = 195.7$; Group 2: $m_1 = 15.1, p_b = 189.3$; Group 3: $m_1 = 13.9, p_b = 196.2$; Group 4: $m_1 = 14.0, p_b = 197.3$.